

# Recent Advances in Development of New Technology in Pre and Intra Operative Breast Cancer Diagnoses

Justina A Ugwah<sup>1,4</sup>, Martin O'Sullivan<sup>2</sup>, Brian O'Donnell<sup>3</sup>, Eric J. Moore<sup>1,4\*</sup>

<sup>1</sup>Life Sciences Interface, Tynadall National Institute, University College Cork, Ireland

<sup>2</sup>Department of Surgery, Cork University Hospital, Cork

<sup>3</sup>Department of Anaesthesia, Cork University Hospital, Cork

<sup>4</sup>School of Chemistry, University College Cork

## Article Info

### Article Notes

Received: March 23, 2021

Accepted: May 27, 2021

### \*Correspondence:

\*Dr. Eric J. Moore, Life Sciences Interface, Tynadall National Institute, University College Cork, Ireland;  
Email: e.moore@ucc.ie.

© 2021 Moore EJ. This article is distributed under the terms of the Creative Commons Attribution 4.0 International License.



### Keywords:

Breast cancer

Techniques

Margin assessment

## ABSTRACT

Breast cancer is the second most occurring malignant disease in women. 1 in 9 women will be affected by this disease in their lifetime. The gold standard for breast cancer screening is the mammographic technique, which has its limitations especially for women aged below 40 as a result of breast density. Ongoing research are exploring techniques that can improve detection accuracy as well as reduce time and money spent in advanced stage treatment options. This review paper highlights the different technologies that have been developed for breast cancer diagnoses.

## Introduction

Breast cancer screening is a process that requires a relatively non-invasive test, with reasonable sensitivity, applied to a wide target population<sup>1</sup>. Diagnostics kick in when the screening process identifies abnormalities that require further evaluation. The breast cancer Ireland estimates that 1 in 9 women will be affected with breast cancer in their lifetime. Current statistics in Ireland show that 5-10% of breast cancer cases are hereditary. 30% of women are diagnosed between 20-50 years, 34% of women are diagnosed between 50-69 years and 36% of women are diagnosed over the age of 70 years<sup>2</sup>. The screening age for Breast Check in Ireland is 50 years, women below this age who make up 30% of total diagnoses will not have the disease detected early. If the diagnosis is ductal carcinoma in situ (DCIS), a non-palpable type of cancer, it cannot be detected by normal physical examination. Though the mortality rate in Ireland has decreased by 2% and survival rate improved by 85% as a result of the screening services and awareness<sup>3</sup>.

Tumours arise from abnormal cells that acquire uncontrolled proliferation and extensive differentiation abilities<sup>4</sup>. Normal and malignant cells create tumour microenvironment that is heterogeneous among patients. These tumours have different hormonal and molecular properties and so require a myriad of diagnostic methods to diagnose them. There are numerous breast screening methods; the clinical breast exam (CBE) and mammography are the two most extensively applied techniques<sup>5</sup>. The gold standard for breast cancer screening is mammography (MG), with a histological assessment of biopsy obtained used for definitive assessment. MG, though a very effective technique in screening for older women has not been very effective in women under 40 years. This is because of higher breast density breast

found in younger women. It also has a high false negative ratio which varies from 4% to 34%<sup>6</sup>.

Breast-conserving surgery (BCS) is the recommended standard of care for women with early stage malignancies<sup>7</sup>. BCS in oncological treatment aims to remove the tumour and preserve as much healthy breast tissue as possible. Despite preoperative imaging modalities such as CT and MRI, intraoperative identification of breast cancer tissue can be challenging. Not with standing major improvements in preoperative imaging, real-time intraoperative imaging modalities are still lacking. A main challenge of BCS is the detection of tumour margins. Breast cancer surgeons still rely on palpation and previous MG, breast Ultrasound, US or MRI to determine the extent of resection. Previous studies reported that the incidence of tumour cells at or near the cut edge of the surgical specimen ranged from 5% to 82%<sup>8-14</sup>. Inadequate margins in BCS are associated with an increased possibility of local recurrence of breast cancer. Majority of the studies also suggest positive resection margins in 20% to 40% of patients after resection of the primary tumor<sup>8</sup>. Current pathological methods require protracted sample preparation procedures. This makes intraoperative assessment of the entire resection surface impractical during surgery. Re-excision surgery also causes substantial physical, psychologic, and financial burdens for patients. There is higher risk of complications with worse cosmesis and additional costs<sup>15</sup>. Intraoperative detection of tumour at the margins would allow more complete resection of malignant tissue in the first operation. It will provide confidence to the surgeon that no residual cancer remains in the breast<sup>16</sup>. Implementation of an accurate intraoperative margin assessment tool may reduce this re-excision rate.

Intraoperative ultrasound guidance of excision has been shown in a small number of studies to reduce re-excision rates by more than half for invasive cancers<sup>17, 18</sup>. However, ultrasound is operator-dependent and has limited reliability for visualizing *in situ* or multifocal cancers<sup>19, 20</sup>. There are two feasible methods for Intra-operative margin assessment. One is by analysing the surfaces of the resection cavity *in vivo*, which is particularly challenging. An easier method is the assessing of the margins of the resected (*ex-vivo*) specimen. At present there is no real-time non-destructive intraoperative technique to assess the microscopic status of lumpectomy margins as standard of care. Frozen section analysis (FSA) is one technique which has been proposed but has not widely been accepted as part of standard of care. This is due to difficulties in performing frozen sections on adipose tissue. It has an added time (~20-30 minutes) to the surgical oncological workflow and additional pathology evaluation with increased costs. The most significant disadvantage is the inability for FSA to be performed over the entire surface area of the

tissue specimen. FSA also shares the same sampling rate limitation as Paraffin section analysis (PSA). They both sample only 10-15% of the surface area<sup>21</sup>. Also, the current use of visual or x-ray examination of excised mammary tissue are not adequate in diagnostic accuracy. Optical imaging using exogenous contrast agents could usher in a new era in surgical oncology.

Thus, it is imperative that new technology to identify breast cancer tissue intraoperatively be developed. This review looks at some of the techniques that are being used to develop new technologies with potential to improve breast disease diagnosis. It discusses which of the technology is commercially available, their limitations and how they fit into the breast lesion diagnostic pathway.

## Techniques

### Mass spectrometry

Mass spectrometry (MS) is an innovative addition to the field of margin detection technologies. Molecules are analysed by measuring the mass-to-charge ratio ( $m/z$ ) of molecular ions and their charged fragments. MS is well proven tool for quantifying small molecules and is also valuable for identifying metabolites and biomarkers<sup>22</sup>. Tandem Mass Spectrometry, MS/MS has been used to characterise key lipid species present in normal and cancerous breast tissue. It has been reported that breast cancer demonstrates metabolic profiles that are distinct from those metabolic profiles found in normal breast tissue. This finding suggests a potential for using metabolite information for breast cancer diagnosis and tumor margin identification<sup>23-25</sup>. A variety of MS platforms including matrix-assisted laser desorption/ionisation (MALDI) and desorption electrospray ionisation (DESI) show promise in differentiating tissue types. They have the potential in applications for rapid tissue diagnostic<sup>25-27</sup>. Mass spectrometry imaging (MSI) can use lipidomic information to distinguish cancerous from noncancerous tissue as well as define tumor margins. It has been successfully applied for molecular imaging of cancer tissues<sup>28-30</sup>.

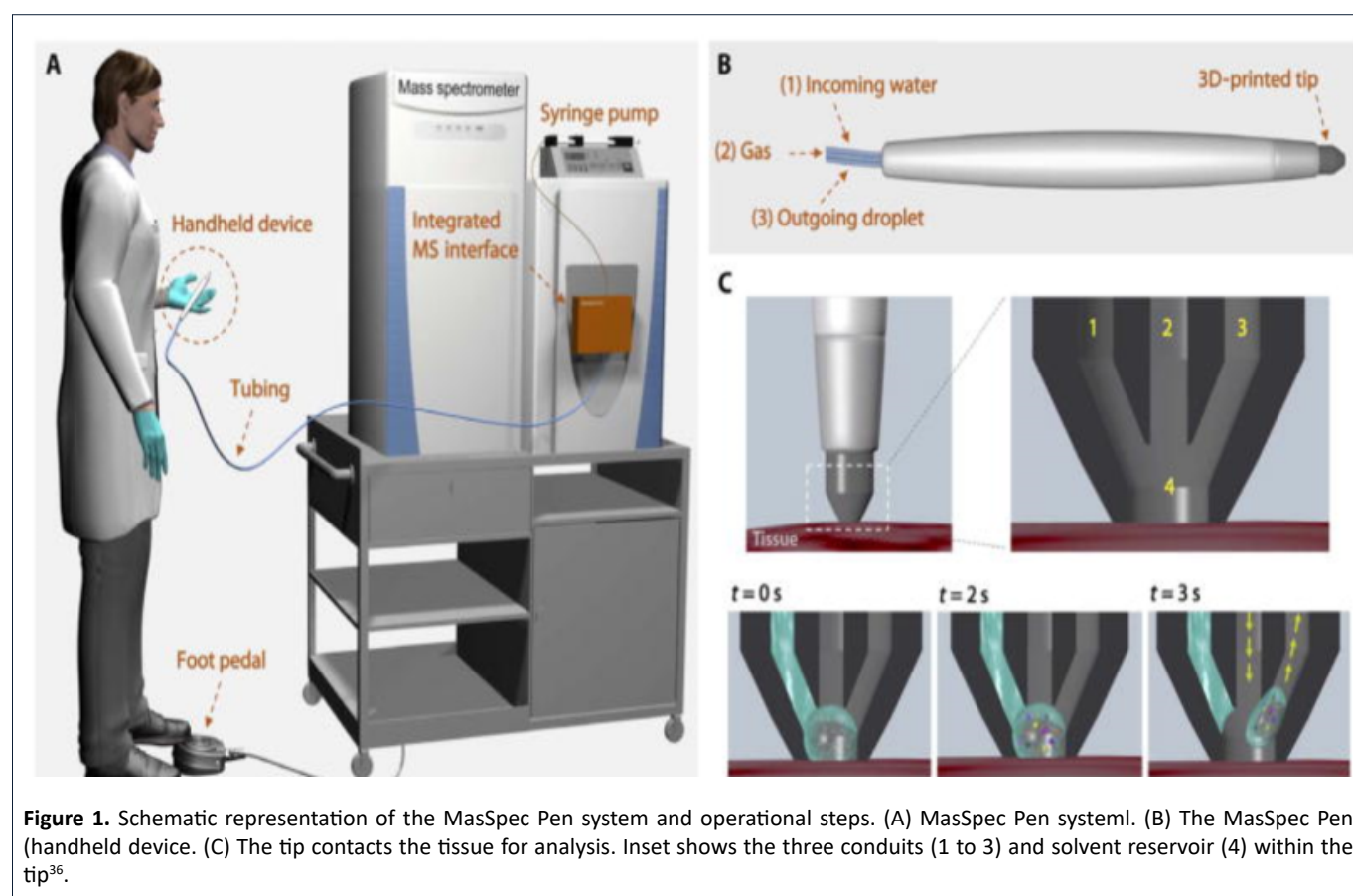
In DESI-MSI, a highly charged aerosol is sprayed onto a surface. The desorbing and ionizing molecules are then analyzed by MS. Samples are analyzed in their native conditions with minimal to no sample preparation (e.g., without the need for separation or an organic matrix). Chemicals, drugs, metabolites and lipids are rapidly detected and mapped in diverse types of samples<sup>31</sup>. The utilization of a spray of organic solvents, high-pressure nebulizing gas, and high voltage have prevented the use of DESI-MSI in *ex-vivo* and *in vivo* analyses. Rapid evaporative ionization MS, or the iKnife, which will be discussed later is an approach which uses MS. It merges an electrocauterization device with MS for tissue discrimination and has been successfully in *in-vivo* malignancy diagnosis<sup>32, 33</sup>. Ultraviolet

and infrared lasers coupled with MS has also been used for characterization of cancer tissue<sup>34,35</sup> These approaches are advantageous in integrating common surgical methods into an MS-based diagnostic workflow. Their limitation lies on tissue damage when molecular ions are produced and being restricted to a specific surgical modality.

Zhang *et al* in their work developed a MasSpec Pen which is automated and biocompatible. It is a handheld sampling probe for direct, real-time, non-destructive sampling and molecular diagnosis of tissues. It is important to note that the chemical extraction used by this process is non-destructive. In figure 1A, the pen-sized handheld device is integrated into a laboratory-built MS interface through a PTFE tubing. The integrated MS interface houses the pinch valves, microcontroller, and tubing to connect the system to the MS inlet. The system is triggered by the user through a foot pedal. The PDMS probe tip is disposable and designed with three PTFE ports. An incoming port delivers a single water droplet to the probe tip (conduit 1). The central port is for gas (N<sub>2</sub>, CO<sub>2</sub>, or air) delivery which is conduit 2. The outgoing port is to transport molecular constituents in the water droplet from the tissue to the mass spectrometer (conduit 3). At the probe tip, all ports combine into a small reservoir where a single water droplet is retained and exposed to the tissue sample. This is done for a controlled amount of time (3 s),

allowing efficient analyte extraction. When the system is triggered ( $t = 0$  s) by using the foot pedal, the syringe pump delivers a controlled volume of water to the reservoir. The discrete water droplet interacts with the tissue to extract the molecules ( $t = 2$  s). After 3 s of extraction, the MasSpec Pen is removed from the tissue. The vacuum and the gas conduits are simultaneously opened, shown in figure 1C (arrows). The conduit 3 is opened to allow the transport of the droplet from the probe to the MS through the tubing system for molecular analysis<sup>36</sup>. This is done at a positive pressure from a low-pressure gas delivery<sup>36</sup>. The gas provided by the second tube does not participate in the extraction process. It is used to prevent the collapse of the system because of the vacuum and to assist solvent transport from the tissue to the MS. As seen in figure 1, subsequent flush step cleans the system; this is not used for extraction of biomolecules from tissues because there is no contact with the tissue during this period. Conduit 3 is directly connected to the transfer tube of a high-mass resolution Orbitrap MS. The negative pressure of the MS vacuum system drives the movement of the droplet from the reservoir to it for ionization and mass analysis.

The mass spectra study by Zhang *et al* was obtained from the analysis of 20 thin tissue sections and 253 human tissue samples<sup>36</sup>. The results presented a rich molecular library of the breast disease state. The MasSpec pen with



lasso prediction results for breast tissue of normal versus cancer achieved 87.5% sensitivity, 100% specificity, 95.6% accuracy and an AUC of 1. The mass spectra obtained presented rich molecular profiles characterized by a variety of potential cancer biomarkers identified as metabolites, lipids, and proteins which most of the other technologies that will be discussed do not provide.

The technique used by the MasSpec is a surface measurement with spatial resolution for each measurement. This is limited by the small pen tip diameter (1.5 mm). Clinically, the MasSpec Pen could be suitable for pre- and post-surgical procedures that require diagnosis of ex vivo samples (fresh or section tissues or biopsies) commonly examined by pathologists<sup>36</sup>.

### Rapid evaporative ionization mass spectrometry

Rapid evaporative ionization mass spectrometry (REIMS) is a real time technique that has used to characterize human tissue. It is achieved by measuring the mass-to-charge ratio ( $m/z$ ) of aerosolized charged particles during electrosurgical dissection. It is then compared to chemical changes in cellular metabolism. MS/MS has been used to characterise lipid species present in healthy and malignant breast tissues. Report findings by a few groups have shown abundance of ions associated with phospholipid species (600–850  $m/z$ ) are increased in cancer tissues compared to healthy tissues. Intensity of ions associated with triglyceride species

(850–1000  $m/z$ ) are decreased. Sakai et al and Sabine et al reported same findings using alternative techniques<sup>22,37,38</sup>. In REIMS, the aspiration of the aerosol allows for rapid mass spectrometric chemical analysis. Computational algorithms can “learn” (cf. ‘machine-learning’) to recognise the chemical differences between tissue types. Balog et al in their work leveraged the technology to identify tissue characteristics in a few seconds of electrosurgical activation<sup>33</sup>. REIMS aims to avoid disruption to surgical workflow and deliver results fast. It allows a surgeon to make decisions regarding tissue resection in real time without worrying about retrospective tissue orientation. It is the technique used by the iKnife.

Intelligent knife, iKnife offers a reliable, effective, and rapid intraoperative margin assessment system for neoplastic tissue characterization. Its accuracy is competitive with standard histological assessment. It can guide in vivo resection, hence, improving quality in breast surgical oncology<sup>22</sup>. St. John et al in their study demonstrated the proof of concept that iKnife is capable of intraoperative analysis of electrosurgical vapours<sup>22</sup>. They trimmed breast tissue samples to size (3–10 mm<sup>2</sup>) and made between 1 to 10 small cuts through the tissue. This was done using a modified monopolar blade electrosurgical pencil (Medres, Hungary) in either the pure *cut* setting (continuous RF wave) or *coagulating* (pulsed RF wave) setting with a ForceTriad™ generator (Medtronic, Ireland).

Figure 2A illustrates the ex-vivo recognition workflow

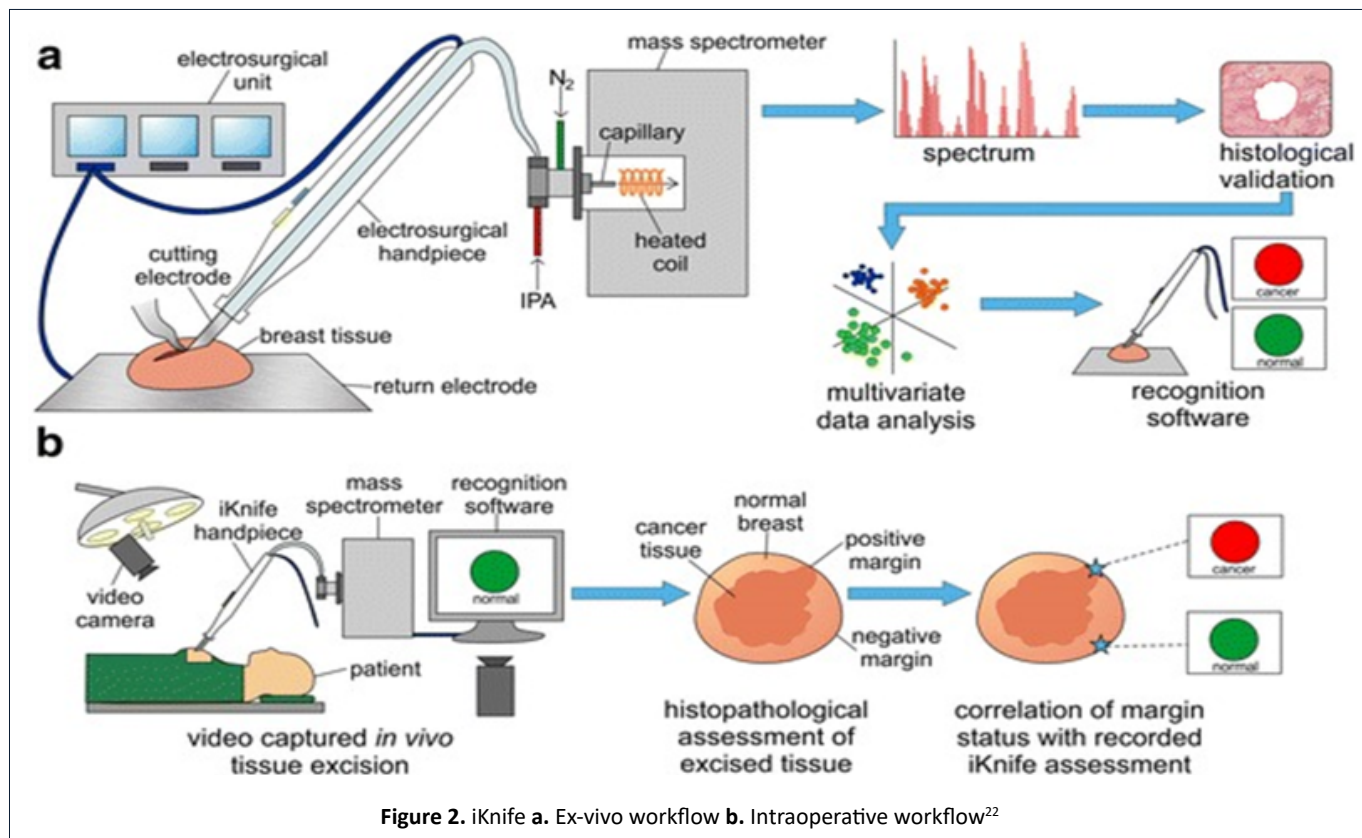


Figure 2. iKnife a. Ex-vivo workflow b. Intraoperative workflow<sup>22</sup>

using the iKnife. It highlights the generation of spectra by the MS after analysis of the surgical aerosol. The model building using multivariate statistics to the *ex-vivo* recognition of the tissue in real time. The figure 2B shows the intraoperative workflow of the iKnife in real time using online MS to the determination of margin status by histopathological assessment and correlation. Aerosol is produced by electrosurgical activation. It is then aspirated via the electrosurgical hand-piece and transferred through a plastic tube to the MS using a Venturi air jet pump. Surgical aerosol is co-aspirated with propan-2-ol at 0.2 ml per minute into the vacuum system of the quadrupole time-of-flight MS. The aerosol particles and solvent droplets are de-clustered using a heated jet disruptor surface in the coarse vacuum region. Gaseous negative ions then enter the MS ion optics for mass analysis<sup>22</sup>. St John et al in their study used samples with adequate spectra, representative of true pathological change to build the tissue-type MS database<sup>22</sup>.

The iKnife is envisaged to be more than just an intraoperative margin assessment tool. This is possible because the iKnife has the margin control device coupled to the resection tool. This is an advantage as the exact orientation of resected breast specimen can prove challenging and affect accurate margin identification. It has the potential to provide real-time chemical information about individual tumour biology. This is essential in an era of precision medicine as we move towards personalized treatments based on tumour/tissue biology<sup>39</sup>.

REIMS is a destructive process; therefore, it is impossible to be certain of the histology of the exact cells under analysis. The iKnife has an exclusion criteria of tumours of macroscopic size  $\geq 2$  cm to enable adequate examination of tissue without compromising clinical diagnosis. The iKnife has relatively low resolution and may lead to dilution of tumour cellular content by normal cells as a result of the width of the electrosurgical blade (4 mm). This could then trigger a false positive result<sup>22</sup>. Results with the iKnife may be obtained fast enough to alter tissue excision in real time and hence, reduce problems with retrospective tissue orientation. In spite of additional factors like blood flow and body temperature, the iKnife obtains high intensity mass spectral data *in-vivo*. This is comparable to the data also obtained in the *ex-vivo* study.

## Raman Spectroscopy

Raman spectroscopy is an inelastic scattering process in which photons incident on a sample transfer energy to or from molecular vibrational modes<sup>40</sup>. It is a coherent two-photon process in which a molecule simultaneously absorbs an incident photon and emits a Raman photon. This is accompanied by its transition from one energy level to another, giving rise to a frequency (i.e., energy) shift of

the emitted photon. Raman spectra are chemical-specific because the energy levels are unique for every molecule. Individual bands in the Raman spectrum are characteristic of specific molecular motions<sup>41</sup>. Raman spectroscopy is particularly amenable to *in vivo* measurements, because the powers and excitation wavelengths that are used do not affect the tissue. The penetration depth is also relatively large<sup>42</sup>.

Surface-enhanced Raman scattering (SERS) using targeted nanoparticles (NP), for multiplexed imaging of cancer biomarkers has been proposed as a technique. This focuses a laser on a sample and measures scattered light to determine a frequency shift. Based on the shift, a unique vibrational spectrum is identified. Every biological molecule has its own tissue biochemical composition which can be determined by a distinctive Raman spectrum.

Wang et al assessed the diagnostic accuracy of Raman-encoded molecular imaging (REMI) for identifying carcinoma at the surfaces of freshly excised breast specimens<sup>43</sup>. They used REMI with SERS-NP to simultaneously quantify four cell-surface biomarkers -: human epidermal growth factor receptor 2 (HER2), membrane estrogen receptor (mER), epidermal growth factor receptor (EGFR) and CD44. For tumor detection, Haematoxylin and eosin (H&E) histology was used as a gold standard. They showed that *ex-vivo* tissues dissected from mastectomy and lumpectomy specimens showed promising sensitivity (89.3%) and specificity (92.1%) for cancer detection. The technique is conducive to personalized biomarker imaging based on tumor-specific molecular profiles<sup>44</sup>. Depending on the sample size, their entire, REMI procedure (staining, rinsing, imaging, spectral demultiplexing) was performed within 10–15 min<sup>44</sup>.

SERS NP were functionalized with different monoclonal antibodies (mAb) targeting either of the four biomarkers. Negative-control NPs were also prepared by conjugating one NP flavor with an isotype control antibody (mouse IgG1). The NPs, functionalized with active thiols at their surface, were first reacted with a fluorophore, DyLight 650 Maleimide. This was done for the purposes of flow-cytometry characterization. The NPs were then conjugated with either an isotype control, an anti-EGFR mAb, an anti-HER2 mAb, an anti-ER mAb or an anti-CD44 mAb at 500 molar equivalents per NP.

As seen in Wang et al study in figure 3, freshly resected human breast tissues from lumpectomy procedures are immediately transferred to a pathology suite for intraoperative consultation. Each specimen is topically stained with a mixture of SERS NPs (multiple biomarker-targeted NPs and at least one untargeted control NP (step 1). After 5 min of staining, the tissue sample is rinsed in 50-mL PBS with gentle agitation for 10 s. This is followed

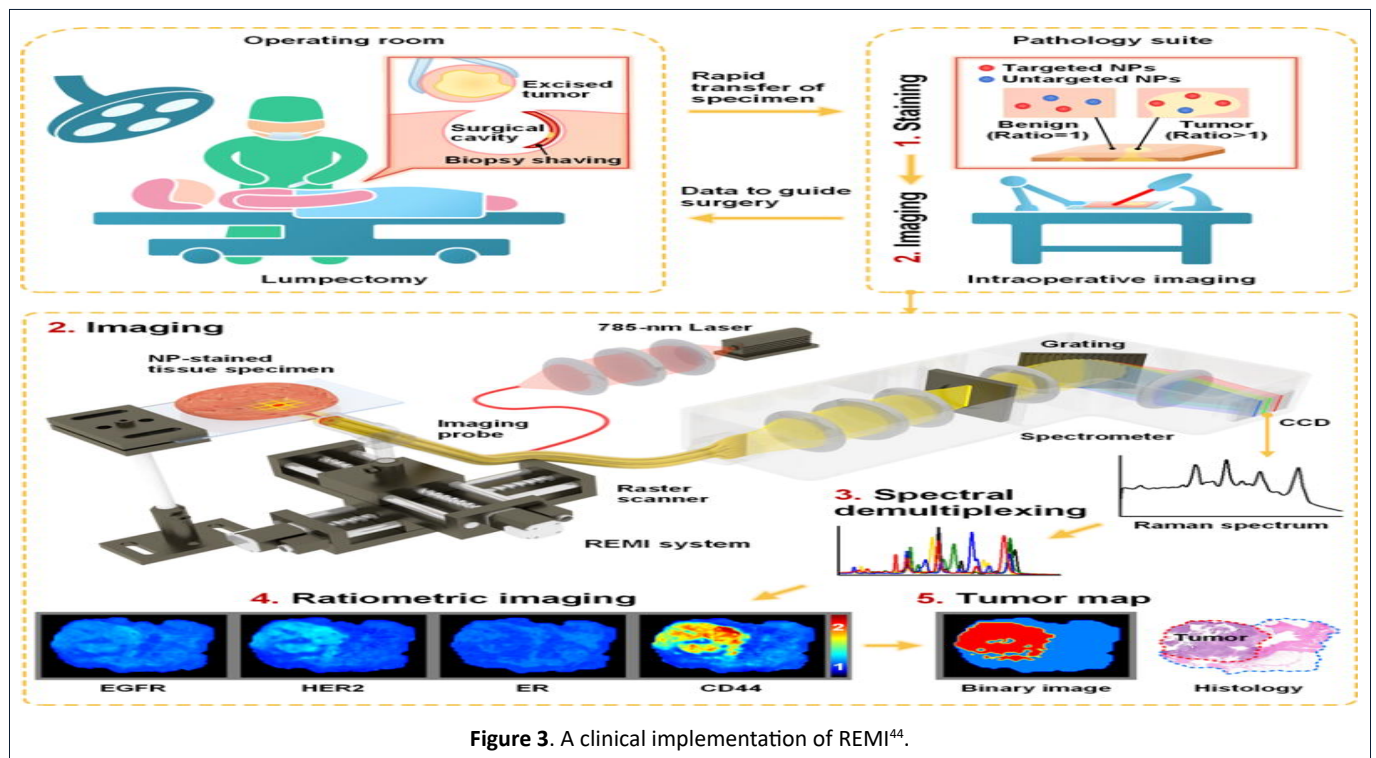


Figure 3. A clinical implementation of REMI<sup>44</sup>.

by spectroscopic imaging at  $>3 \text{ cm}^2/\text{min}$  of the surgical margin surface (step 2). The acquired SERS spectra are demultiplexed at  $\sim 1000$  spectra/s to determine the ratio of the targeted vs. untargeted NPs (step 3). This enables the quantification of various biomarker targets (step 4). REMI images of the individual biomarkers are combined to detect the presence of residual tumors at the surgical margin surfaces of the specimens (step 5). The entire REMI procedure from step 1 - 5 can be performed within 15 min. After imaging, the tissues were fixed with 10% formalin and submitted for histopathology assessment.

The ratiometric imaging approach is a critical component of REMI. This enables accurate and sensitive identification of biomarker over-expression without the confounding effects of nonspecific background signals<sup>44-46</sup>. The imaging of the raw concentration (signal) of targeted NPs fails to differentiate between malignant and benign regions. This is as a result of the nonspecific accumulation of the NPs. This misleading phenomenon at times affect all molecular imaging when exogenous contrast agents are delivered systemically or topically. The imaging of raw NP concentrations (signals) suffers from other effects such as variations in illumination power and detector working distance (for example due to tissue-surface irregularities). Ratiometric imaging is insensitive to these effects<sup>43</sup>.

Shipp et al in their work used a multimodal imaging technique combining tissue auto-fluorescence and Raman spectroscopy<sup>47</sup>. Trained diagnostic algorithms were optimized to quickly evaluate large excised breast tissue surfaces to detect microscopic residual tumor. Independent

tests of 121 samples from 107 patients - including 51 fresh, whole excision specimens - detected breast carcinoma on the tissue surface with 95% sensitivity and 82% specificity. This was done. The analysis time can be further reduced by optimizing and automating instrument to eliminate the current manual steps (e.g. microscope focusing, change between AF and Raman objectives, and faster microscope translation stage<sup>47</sup>.

In the REMI with topically applied SERS nanoparticles technique, its capability can be enhanced by exploiting machine learning methods to identify tumor regions precisely based on unique biomarker expression signatures. This is more acceptable rather than the assumption a tissue region is malignant if any of the biomarker targets is overexpressed. A major capability of the REMI method lies in its ability to detect carcinoma where a previously expressed biomarker is no longer present. The absence of the biomarker could be as a result of either neoadjuvant treatment or natural disease progression<sup>44</sup>. It is comparable to current intraoperative guidance techniques such as FSA. FSA typically requires 15-30 min but suffers from sampling errors and freezing artifact due to the high lipid content in breast tissues while raman techniques typically have low scanning speeds (12-24 minutes).

### Near-infrared fluorescence imaging and methylene blue

Near-infrared (NIR) light, in the wavelength range of 700 to 900 nm, offers several significant advantages over presently available imaging techniques. This includes

relatively high photon penetration into and out of living tissue. This penetration is due to reduced absorbance and scatter with a relatively high signal-to-background ratio (SBR) due to low tissue autofluorescence<sup>48</sup>. In order to use NIR, a clinical-grade intraoperative fluorescence imaging system and a tumor-specific NIR probe are mandatory. NIR fluorescence imaging is a surface technology ( $\approx 5$  mm penetration depth). NIR fluorescence has an exceptionally high spatial resolution compared to conventional imaging techniques. NIR fluorescence imaging has the potential to address a variety of unmet clinical needs These needs relate to finding structures that need to be respected, such as sentinel lymph nodes, malignant cells, and luminal calcifications. Also avoiding other structures like nerves, blood vessels, ducts, lymphatics, and normal glands that could cause acute or chronic morbidity during BCS<sup>49</sup>. There are factors which need to be optimised to benefit from the full potential for NIR fluorescence imaging. They include concentration of the NIR fluorophore in the target tissue, minimizing the photon absorption and scattering in the tissue, maximizing excitation power of NIR excitation without inducing photobleaching or photo damage to

tissue and the sensitivity of the Charge Coupled Device (CCD) chip on the detector.

Sentinel lymph node (SLN) mapping is one of the most promising clinical applications of NIR fluorescence imaging in the field of oncology. There have also been recent clinical results using intra-operative NIR fluorescence cameras<sup>48, 50</sup> or portable NIR-imaging devices<sup>51</sup> in SLN mapping. NIR fluorescence imaging is a promising technique that can be used not only for intraoperative identification of sentinel lymph nodes but also tumors and vital structures<sup>52</sup>. Multiple camera systems have become clinically available, however FDA/EMA approved tumor-specific probes are still lacking.

Technetium(<sup>99m</sup>Tc)-sestamibi (MIBI) is a lipophilic cation used for preoperative, non-invasive identification of malignant tissue via SPECT imaging[53]. Preoperative identification of breast cancer is possible in approximately 83–90% of patients using <sup>99m</sup>Tc-MIBI<sup>53-55</sup>. The clinical understanding of <sup>99m</sup>Tc-MIBI in breast cancer imaging is used to discriminate between malignant and benign lesions. Therefore, it is important to exploit other clinically

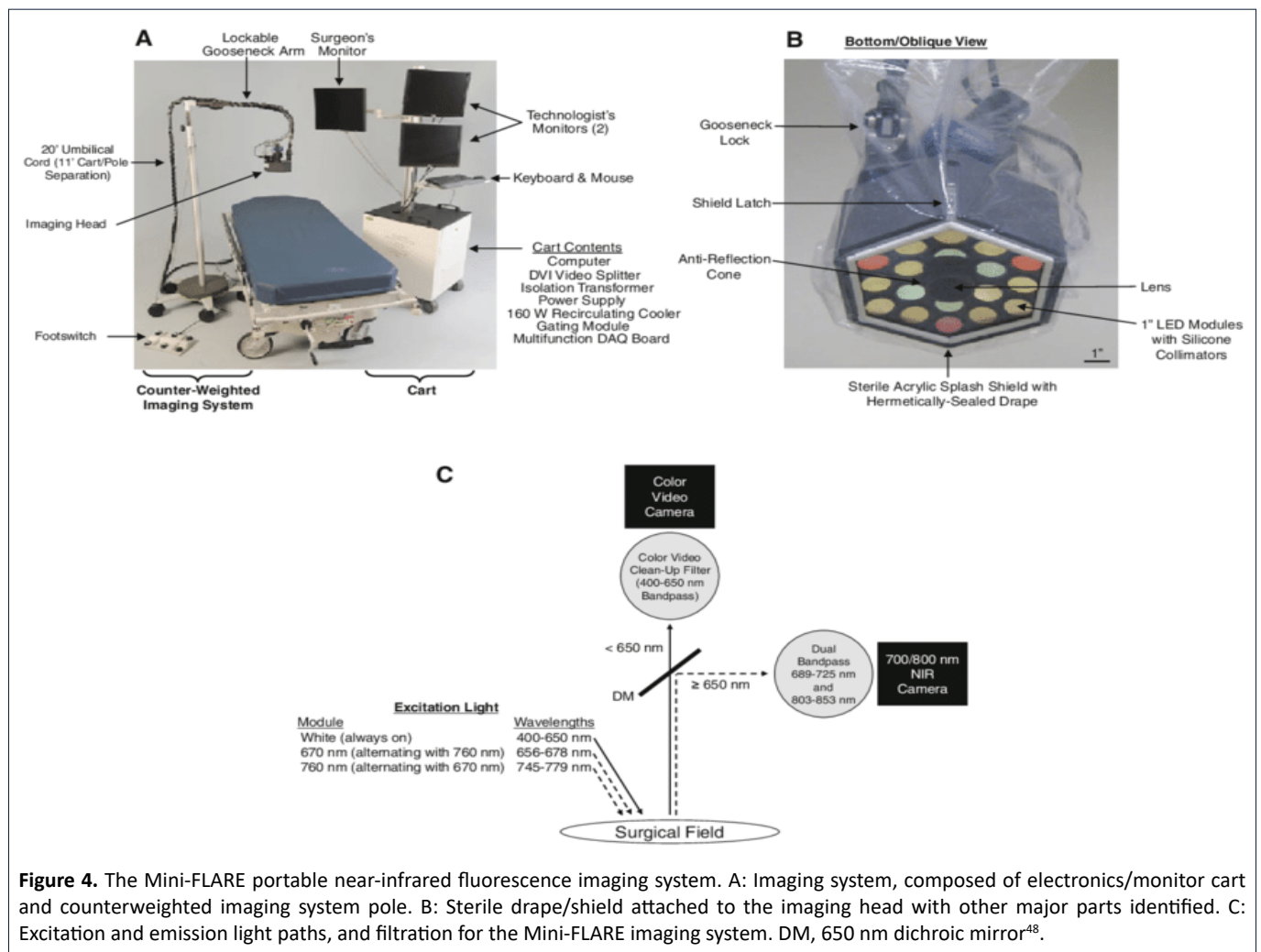


**Figure 4.** The Mini-FLARE portable near-infrared fluorescence imaging system. A: Imaging system, composed of electronics/monitor cart and counterweighted imaging system pole. B: Sterile drape/shield attached to the imaging head with other major parts identified. C: Excitation and emission light paths, and filtration for the Mini-FLARE imaging system. DM, 650 nm dichroic mirror<sup>48</sup>.

available contrast agents, such as indocyanine green (ICG) and methylene blue (MB)<sup>56</sup>. Tummers et al in their work used Methylene Blue (MB) because of its physiochemical similarities with <sup>99m</sup>Tc-MIBI<sup>57</sup>. They used it for identification of breast tumor intraoperatively to compare early and delayed imaging protocols<sup>57</sup>. MB has been determined previously to be an effective NIR fluorophore. It can function as a perfusion tracer *in vivo*<sup>58,59</sup>. Tummers et al imaging procedures were performed using the Mini-Fluorescence-Assisted Resection and Exploration (Mini-FLARE) image-guided surgery system<sup>60</sup>. It was the first feasibility study with MB in breast cancer. They used a low dose of MB (0.5–1 mg/kg) as the fluorescent tracer.

The Mini-FLARE™ imaging system was developed by Troyan et al in their study<sup>48</sup>. It was done in consultation with surgeons, who had advised that it has become evident that a general-purpose optical imaging system for surgery was needed. The system was required to show the invisible NIR fluorescent light in the context of surgical anatomy<sup>48</sup>. This means that it had to be overlaid onto the color video image. Also required is two independent channels of NIR fluorescent light for procedures that, for instance, require resection of one tissue (such as a tumor) and as well as avoidance of other tissues (such as nerves and blood vessels)<sup>48</sup>. The Mini-FLARE™ imaging system developed by Troyan et al represents a significant reduction in size and improvement in flexibility. The FLARE system consists of 2 wavelength isolated light sources, a “white” light and a NIR light. Color video and NIR fluorescence images are simultaneously acquired and displayed in real time. This is done using custom optics and software that separate the color video and NIR fluorescence images. A pseudo-colored (lime green) merged image of the color video and NIR fluorescence images is also displayed. The imaging head is attached to a flexible gooseneck arm, which permits positioning of the imaging head at extreme angles virtually anywhere over the surgical field. For intraoperative use, the imaging head and imaging system pole stand are wrapped in a sterile shield and drape.

Tummers et al in their study, divided 24 patients into 2 equal administrative groups. The groups, differed with respect to the timing of MB administration. Each patient per group was administered 1.0 mg/kg MB, intravenously over 5 minutes. This was performed, either immediately before surgery or 3 h before surgery. First scheduled patients on the day’s surgical program were administered MB immediately before surgery (early imaging). Patients scheduled later in the day, were administered MB, 3 hours before surgery (delayed imaging). The mini-FLARE imaging system was used to identify the fluorescent signal during surgery and on post-resected specimens transferred to the pathology. During surgery, images were obtained, from the surgical field, the resected specimen, and the wound bed

after resection. When fluorescent signal was observed, the surgeon, based on clinical judgment, could resect or not the fluorescent tissue. The resected specimen was sliced at the pathology department, where images of bisected tumour obtained. When possible, snap frozen tissue were collected for fluorescence microscopic imaging. After slicing of the resected lesion, fluorescent imaging was again performed with the mini-FLARE imaging system.

Tummers et al in 83% of the patients, using the NIR fluorescence imaging of the resected specimen, identified breast tumours (carcinoma in  $n=21$  and DCIS in  $n=3$ ). The imaging was carried out after bisection in the Pathology department. Tumors were identified as a bright fluorescent spot in the sliced specimen. Their analysis also highlighted that patients with non-detectable tumours were significantly older (mean age 68 years old versus 58 years old;  $P=0.03$ ). Both infiltrating ductal and lobular type adenocarcinoma were detectable. No fluorescent tumour was found in patients with mucinous adenocarcinoma or primary mucoepidermoid carcinoma. No significant relation was found with regards to receptor status or tumour grade.

NIR using a fluorescent modality that utilizes molecular contrast can be used intraoperatively to highlight cancer. The optical properties of NIR fluorescence are especially suited for the visualization of possible residual tumor cells at the resection margin. As discussed earlier, it can potentially assist surgeons to visualize tumor in the cavity and the excised lump. This technique relies on preoperative, systemic administration of exogenous dyes. It requires extensive dosing and tumor uptake studies which creates potential barriers to clinical translation. MB is a moderate-strength fluorophore when used at low concentrations at an excitation maximum of 670 nm. Contrast agents with an emission peak of  $\approx 700$  nm have several limitations compared to 800 nm fluorophores with respect to quantum yield, penetration depth, and autofluorescence.

Tummers et al work identified tumor demarcation in 83% of patients using NIR fluorescence imaging. This also corresponded to histological presence of tumor. Their study did not explore dose, though their results suggest that a formal study of a higher dose than 1.0 mg/kg, is necessary. They concluded that 17% of tumors not identified using MB was because of the low dose used<sup>57</sup>. This is because tracer accumulation is prolonged in malignant lesions<sup>61</sup>. This is different to MRI of breast malignancies, where malignant lesions tends to enhance but also washout quicker than benign lesions. All these developments will have to be in parallel with development of adequate and manageable intra-operative camera systems<sup>62</sup>. Using intraoperative NIR fluorescence imaging, the inability to image the whole breast for small tumor deposits will hence be addressed. This limitation is as a result of its limited penetration depth.

## Optical coherence tomography

The mechanical properties, structure, and function of tissues are linked and altered by disease<sup>63</sup>. Breast tissues has distinct molecular and optical properties but also exhibits mechanical properties. Clinicians palpate tissues to detect changes in stiffness suggestive of disease. However, palpation is a biased tool as large proportion of breast lesions can be thought impalpable. It can be either too small or soft to detect by touch. Elastography techniques have been utilized to quantitatively image the mechanical properties of tissue. Elastography is a technique that creates images of the mechanical properties of tissue, complementing palpation by visualizing mechanical changes in 2D or 3D<sup>64</sup>. Elastography based on ultrasound has been developed for preoperative diagnosis of breast lesions. It has not been applied to intraoperative margin assessment, largely due to its relatively low spatial resolution<sup>65,66</sup>.

Optical imaging with elastography can be used to probe the breast tissue elasticity, hence, providing accurate assessment of tumor margin involvement. Optical coherence tomography (OCT) is an intraoperative high-resolution imaging technique. It assesses surgical breast tumor margins and provides real-time microscopic images. These images can be up to 2 mm beneath the tissue surface. Unlike ultrasound, it uses light waves as opposed to sound waves. These waves create high-resolution (2-10mm), multi-dimensional images of surface and sub-surface tissue structures. Ultrasound or MR elastography are sensitive to tissue motion measuring displacements of 100s of nanometres to micrometres but OCT is as small as 10s of picometres<sup>67, 68</sup>. OCT produce images with micron-scale resolution. This is at the same level as in histopathology assessment. It can be performed without the need for exogenous contrast agents. It uses interferometry to effectively measure “time-of-flight” of light in tissue. The image is created based on the amount of back-scattered light, with microscopic resolution up to 1- 2 mm in depth[64]. These imaging specifications match

well with the clinical requirements of margin assessment in breast conserving surgery, BCS[16]. OCT is also being used in ophthalmology, cardiology, and gastroenterology<sup>69</sup>.

Allen et al in their work used optical coherence micro-elastography (OCME) to map the local axial strain, at each lateral ( $x, y$ ) and axial ( $z$ ) position, in response to a compressive load applied to the tissue<sup>70</sup>. OCME identifies invasive tumor by heterogeneous patterns in qualitative micro-elastograms. In these cases, strain heterogeneity often arises from localized changes in the mechanical properties between nests of tumor cells and surrounding immature fibrous connective tissue (desmoplastic stroma)<sup>71</sup>. A combination of tumor cells with desmoplastic stroma represents only one micro-architectural pattern in malignant tissue. Invasive tumor may also display homogeneous strain.

Since OCT elastography depends on variation in mechanical properties, it can improve tumour visualization in dense breast tissue. Nguyen et al in their work used OCT to identify areas of homogeneous adipocytes, suspicious regions with highly scattering and tightly packed cells, and heterogeneous scattering patterns. These are also some of the key features used to classify margins as negative or positive in histopathology<sup>72</sup>. As seen in figure 5, light from a SLD ( $\lambda=1310$  nm) is directed into an optical circulator (OC) and to a fibre coupler (FC) which splits 5% of the light to a reference arm mirror (RM) and 95% of the light to a sample arm containing focusing optics and an automated x-y translation stage (TS). Light is collimated through fibre collimators (Col). Reflected light from each arm is coupled through polarization paddles (PP), interfered within the fibre coupler, and spectrally dispersed onto a line camera.

The low contrast between tumor and dense stromal tissue makes it hard for OCT to accurately assess margins. In order to improve this, OCT-based elastography can be employed. OCT elastography measures tissue deformation under an applied load, offering 3D maps of mechanical properties with microscale resolution. Kennedy et al

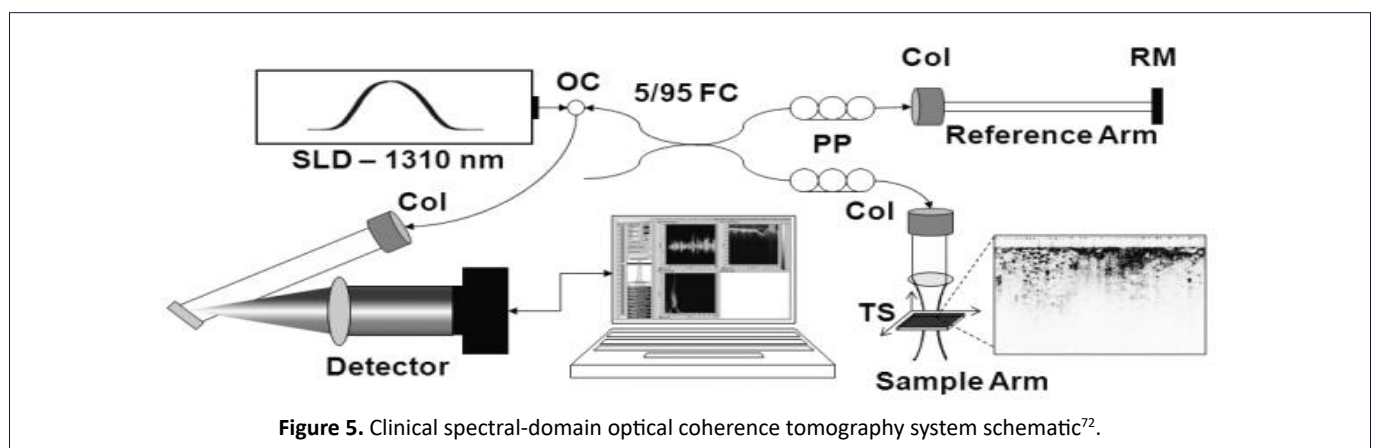


Figure 5. Clinical spectral-domain optical coherence tomography system schematic<sup>72</sup>.

in their study quantified elasticity rather than rely on contrast based on strain alone using wide-field QME. Quantitative micro-elastograms uses compression using optical coherence elastography (OCE) with optical palpation to simultaneously perform strain and stress imaging to produce images of tissue elasticity<sup>16</sup>. They demonstrated the ability to differentiate breast tissue in breast tumours based on elasticity combined with the structural information offered by OCT. Quantitative micro-elastography (QME) can also be used to monitor the response of disease to treatment. It has the potential to image tissue elasticity *in vivo* using handheld probes. Wide-field data volumes of (46 × 46 × 3.5 mm) can be obtained in 10 minutes.

Wide-field (QME) improves visualization of malignant tissue by providing additional contrast. This contrast is based on tissue elasticity and complements the contrast provided by OCT and strain. The advantage is that it removes many of the artifacts present in OCME. As seen in figure 6, the OCT system, the loading mechanism and the wide-field translation stages are the three main elements of the wide field QME. It uses a super-luminescent diode light source with a central wavelength of 1300 nm and a bandwidth of 200 nm. A piezoelectric ring actuator is the loading mechanism and has the imaging window fixed to it. The sample is placed on the compression plate. The compression plate is mounted on three load cells

in triangular alignment. The load cells allow the force applied to the sample before testing to be monitored. The load cells are then mounted on a motorized laboratory jack. This is used to apply preload to sample to bring it in contact with the imaging window. This helps to maximize contact area. The distance travel of the jack determines the maximum thickness of the sample that can be scanned. The individual load cell readings are summed using a custom LabVIEW program. Wide-field datasets are generated by translating the loading mechanism, which includes the sample, silicone layer and imaging window, relative to the OCT scan head between sub-volume acquisitions<sup>70</sup>.

Optimal results can be guaranteed by ensuring full physical contact with the specimen, undamaged tissue by thermal effects (cauterization during resection) and availability of a reliable histology match of region of interest. Micro- to milli-scale non-contact can cause tissue to deform in the opposite direction to the applied load. This will cause strain heterogeneity with similar spatial occurrence as invasive tumor. Therefore, improved mechanical contrast across a wider range of micro-architectural patterns is needed, to increase the clinical utility of wide-field OCT-based elastography. An improvement of QME over OCME is that it reduces artifact caused by surface roughness while maintaining contrast between tissue types<sup>70</sup>.

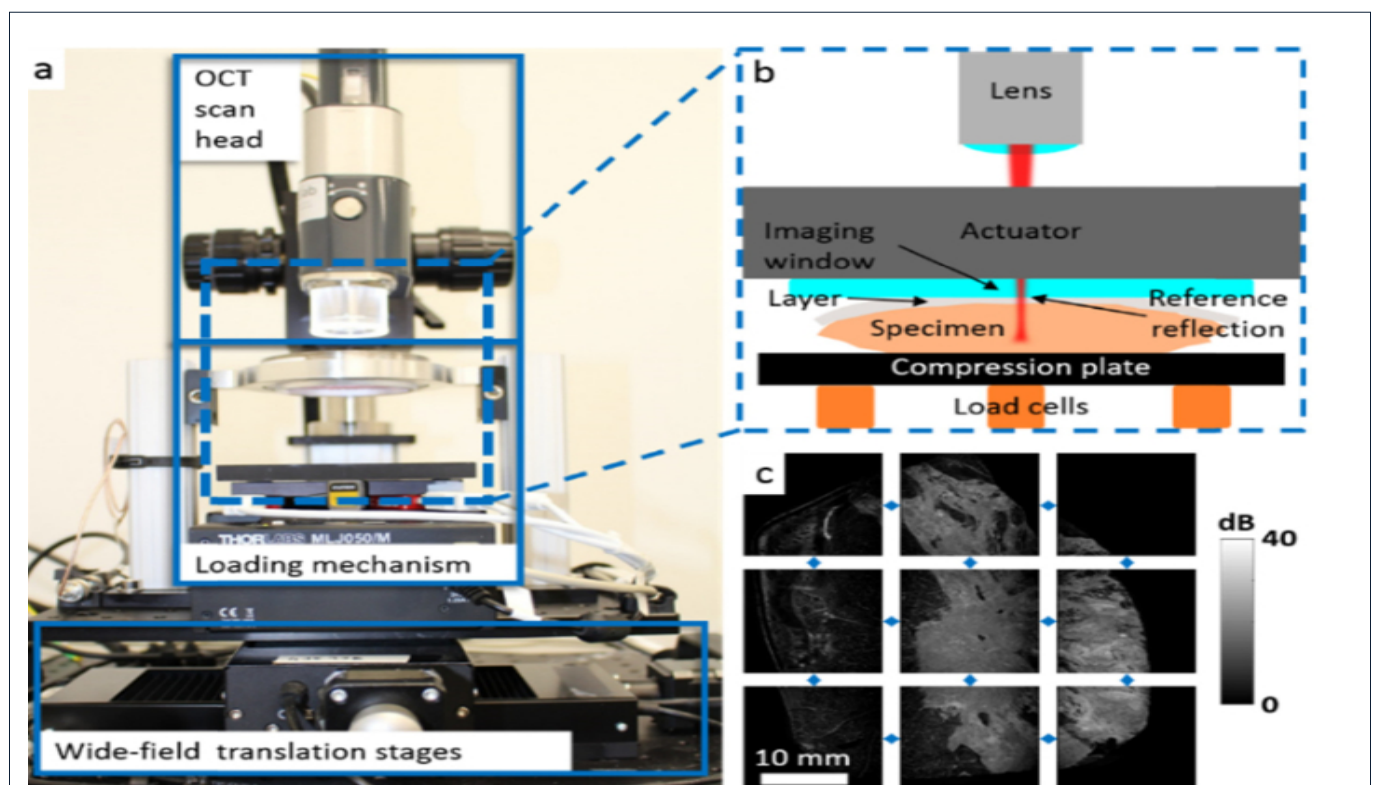


**Figure 6.** Wide-field QME experimental setup. (a) Photograph of wide-field probe with three main elements labeled. (b) Schematic of loaded specimen. (c) Example of unstitched en face OCT images of mastectomy specimen<sup>70</sup>.

## Bioimpedance of breast tissue

In bioimpedance sensing technique, a sensor applies small alternating currents to the sample to assess the tissue resistance over a range of frequencies. This can detect changes in the extracellular and intracellular resistance in tissues that are hallmarks of breast cancer. The development and application of bioimpedance as a technology has been prominent in cancer detection<sup>73-76</sup>. A clear example of this is the ClearEdge (CE). The device comprises of a probe which is used to scan a patient's normal breast tissue. This acts as a baseline and is specific for breast tissue features of each patient. This initial feature assessment is then used to determine healthy versus malignant tissue. It differs from currently available devices because it uses bio-impedance spectroscopy (BIS). BIS is very sensitive to extracellular and intracellular variations of tissue dielectric properties. These variations as well as change in cell size, nuclear size, membrane thickness, pH and ionic content of cells are characteristics that distinguish malignant from normal tissue.

The CE as seen in figure 7A is handheld and a portable imaging device. It is battery operated and has a docking station for charging. This new imaging modality enables surgeons to identify and localize areas of abnormal tissue at a margin based on their dielectric properties.

Tissue abnormalities detected by the device include DCIS, invasive cancer, and also includes abnormalities such as atypical ductal and lobular hyperplasia, lobular carcinoma in situ, and areas of increased cellularity associated with inflammation<sup>77</sup>. DCIS is normally not visible on conventional imaging like mammography or ultrasound.

The surgeon uses the CE to make baseline measurement on each patient's normal breast tissue away from the cancer tissue. In the phase 1 trial study, the safety and accuracy of the device was assessed in ex-vivo specimen. In phase 2 trial, the CE was used intraoperatively to reduce re-excision.

In the trial using the CE, excised specimen was imaged with an X-ray intraoperatively. This image shows if the tumour has been excised. The CE device was used to image each margin of the excised tissue. All margins of the excised tissue and any other cavity margin shavings are scanned multiple times. The CE head's tissue penetration depth guard was set to a depth of 3 mm. This ensured the margins of the excised tumour were free from residual cancer to a depth of 3 mm. A penetration depth of 3 mm in fresh tissue typically corresponds to about 2 mm of fixed tissue as reported by the pathologist<sup>77</sup>. Each scan produces a colour-coded image on the device's LCD display (figure 7B). The surgeon assesses and records each CE image. Orange ink was used to mark sites identified as abnormal by the device. The pathologist examines this area during histology assessment. The anterior, posterior, superior, inferior, medial and lateral margins were assessed in each patient. In Phase-1, re-excision decisions were not made based on the CE assessment. In phase 2, re-excision was performed, if any margin was deemed abnormal by the device. The rate of re-excision was 8% in phase 2 as opposed to phase 1 which was 37%. This reduction was as a result of the surgeon having a better understanding of how to correctly obtain the baseline. Dixon et al in this study demonstrated that CE device had a higher sensitivity than specimen X-Ray<sup>77</sup>. They showed that the CE device

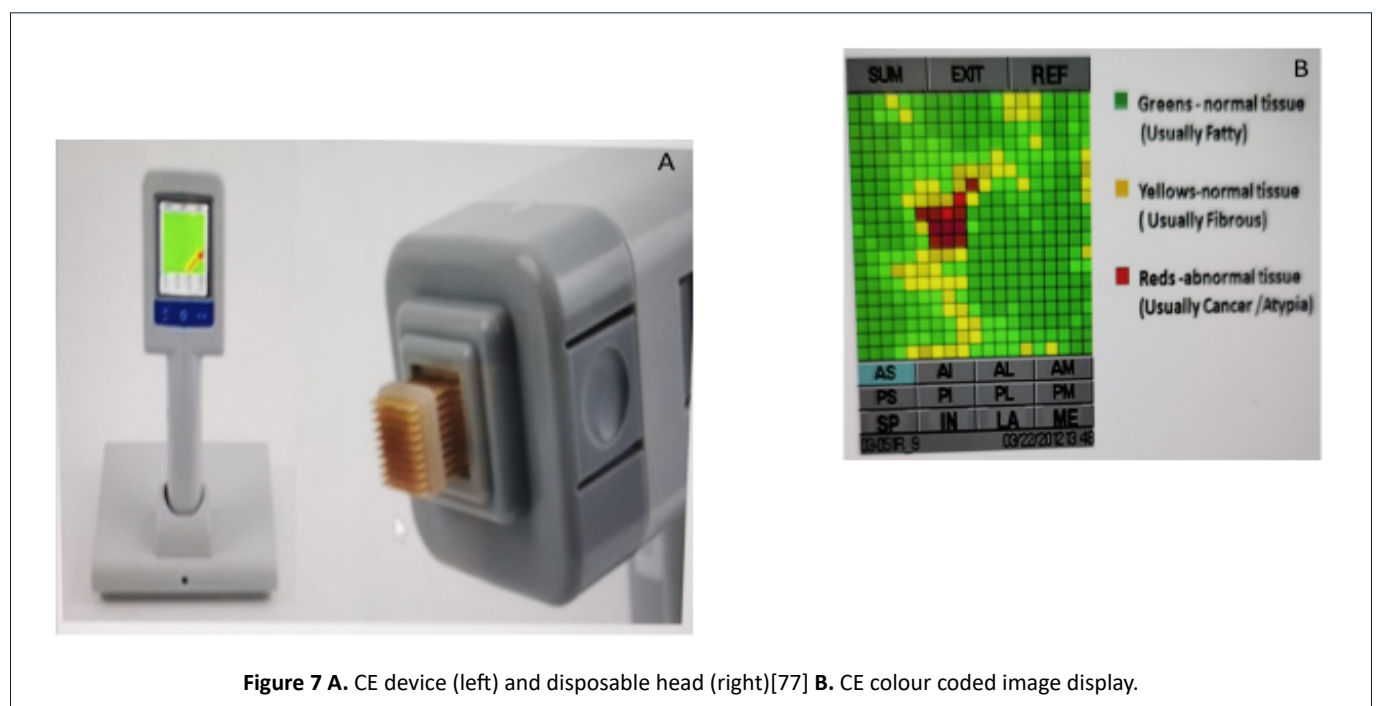


Figure 7 A. CE device (left) and disposable head (right)[77] B. CE colour coded image display.

can identify cancer in dense and fatty tissues. This is an advantage that bioimpedance has over mammography. A challenge that will need to be addressed by the CE device is how to prevent a malignant site or fibrotic tissue being baselined. This could give a false negative result so surgeons must be trained on it extensively.

Bioimpedance as a technique is very fast and can be miniaturised as can be seen in imaging with the CE device. The imaging of all margins took less than 5 min with each image taking only 3 seconds. Though Dixon et al in their phase trials used this to assess breast margins, it can be adapted as an adjunct tool in histological breast cancer assessment.

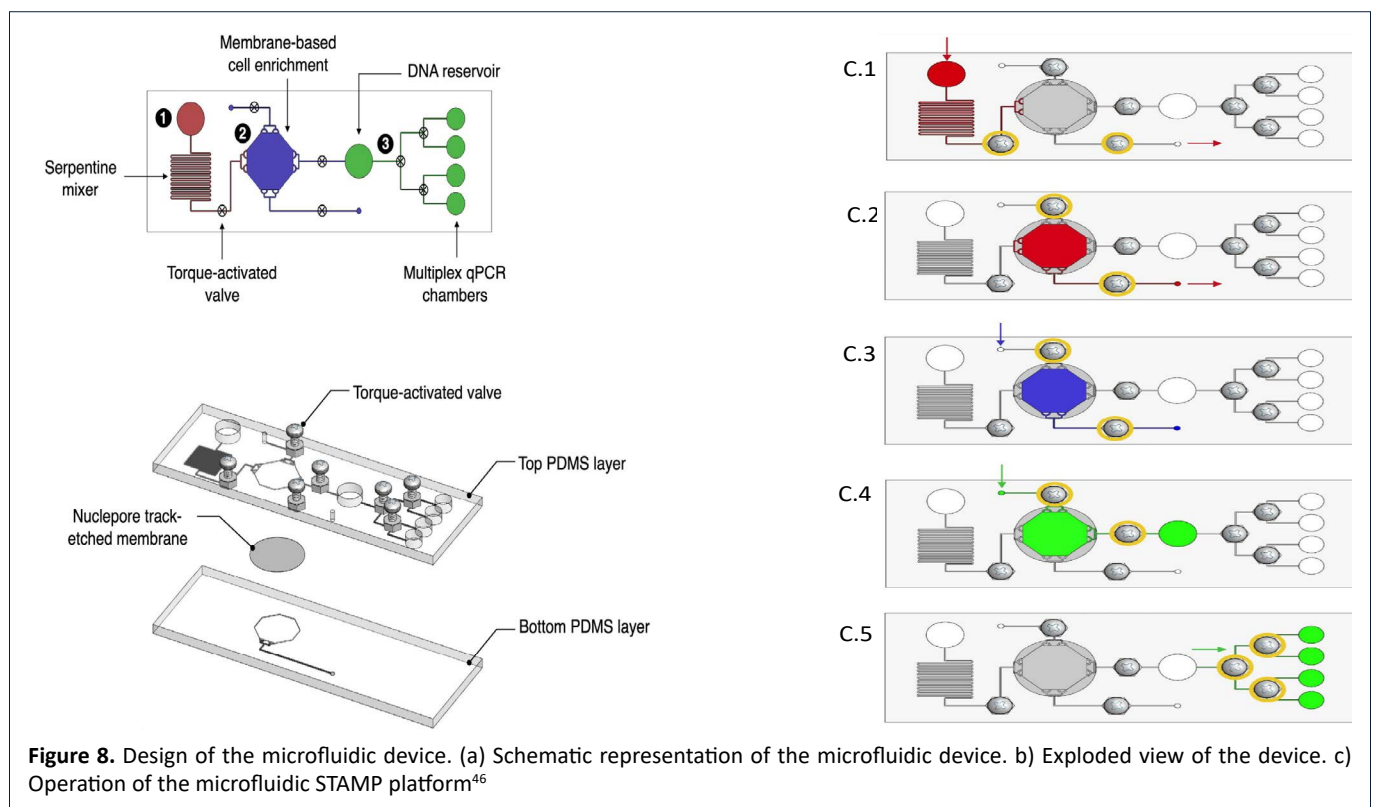
### Sequence-Topology Assembly for Multiplexed Profiling (Stamp)

The analysis of protein expression and distribution holds great potential in discovery of biomarkers. This would enable for early disease detection and improvement in treatment decisions. Definitive diagnosis as well as cancer staging can only be done post-operative. The information obtained, then guides on subsequent treatment for the patient. At present, histopathological assessments can only measure a small subset of protein markers and takes several days with extensive sample processing. Sundar et al in their work have developed a novel technology, Sequence-Topology Assembly for Multiplexed Profiling (STAMP) which will overcome this challenge. The introduction of STAMP in the clinical workflow will enable

early and informative cancer diagnosis. STAMP has high sensitivity and accuracy in detecting and classifying cancer cells to determine the disease aggressiveness from the least invasive biopsies.

STAMP technology takes advantage of the unique properties of DNA to form 3D barcodes. These can be used to measure diverse protein markers and detect their specific locations in cells. STAMP is a more sensitive than current pathological methods. Its advantage lies in providing more information from very small samples. It can be completed in as little as two hours. The 3D barcodes achieve a high labelling efficiency and remain stable against biological degradation.

The STAMP device as shown in Figure 10a consists of three compartments: (1) a serpentine mixer for cell and antibody targeting (red), (2) an embedded membrane (5- $\mu\text{m}$  pore size) for cell enrichment and in situ STAMP barcode generation (blue), and (3) DNA reservoir and multiple chambers for amplification and multiplexed analysis of the generated barcodes (green). The torque-activated valves control fluidic flow from one compartment to the next. The microfluidic device in figure 10b is assembled from two polydimethylsiloxane (PDMS) layers to embed a porous membrane for cell enrichment and STAMP analysis<sup>46</sup>. The five different steps required in the operation of the STAMP platform is outlined in figure 10c (1 - 5). The cellular targeting is the first step where cells are mixed with fixation and permeabilization buffer, which is then introduced into the inlet antibody-DNA



conjugates. The serpentine channel in 10a enhances the mixing to facilitate cellular targeting. Cell capture is the second step where cells are captured on the porous membrane and unbound antibodies are removed via the waste outlet. The third step is the 3D barcode generation, where STAMP reagents, for example DNA tetrahedron probes, localization labels and ligases are introduced to generate 3D barcodes in-situ on cell bound antibodies and these barcodes are then liberated upon heat inactivation of ligase. In the fourth step, barcode amplification, the STAMP barcodes are introduced to the amplification chamber via positive pressure. The barcodes can be pre-amplified with appropriate primers for sequencing analysis or on-chip quantitative polymerase chain reaction, qPCR. In the final step the on-chip qPCR, the STAMP barcodes are transferred to individual qPCR chambers, each preloaded with specific lyophilized primers for real time fluorescence measurements<sup>46</sup>. Using the microfluidic chip of the STAMP technology for diagnoses could cost as low as \$36.

### Margin Probe

Conductivity and Permittivity are two important electrical properties tissue exhibit. Conductivity measures how easily free charges move like a conductor while permittivity measures how bound charges respond like in a capacitor. These properties are reliant on the membrane potential, nuclear morphology, cellular connectivity and vascularity. These properties differ in normal and malignant tissue.

Dune medical devices developed the MarginProbe

as an adjunct technology to measure the local electrical properties in the radiofrequency (RF) range of breast tissue. This has been used in BCS for real time margin assessment. The MarginProbe System is a self-contained system comprising of a probe and a console. The console includes a user interface system with display, audio components and operation buttons<sup>79</sup>. The MarginProbe 1.2 (figure 9A) unlike the earlier version is lighter in weight so portable. It has a brighter screen with a wider viewing angle with improved on-screen notices. Also, unlike the previous model, it has a 90s start-up time and an improved service time.

The MarginProbe System applies an electric field to the tissue through a sensor mounted at the tip of the probe. It analyses the reflection over a wide range of RF frequencies. The Fringe Field Sensor generates an oscillating short-lived electrical field in a small volume (~100 mm<sup>3</sup>) of tissue touching the sensor. It does this by employing the fringe field effect present at the edge of conductors<sup>79</sup>. The field extends into the tissue in the area closest to the sensor, decaying by 90% at 3 mm. The energy applied per measurement is lower than 0.2 mJ, which is an extremely low energy level. The returning signals are altered by the interaction of the fringe field with the tissue in contact with the sensor. They carry with them information regarding the electromagnetic characteristics of the examined tissue. The resonance frequency and amplitude reflection change significantly with change in tissue properties. These parameters are used to characterize tissue as malignant (positive) and

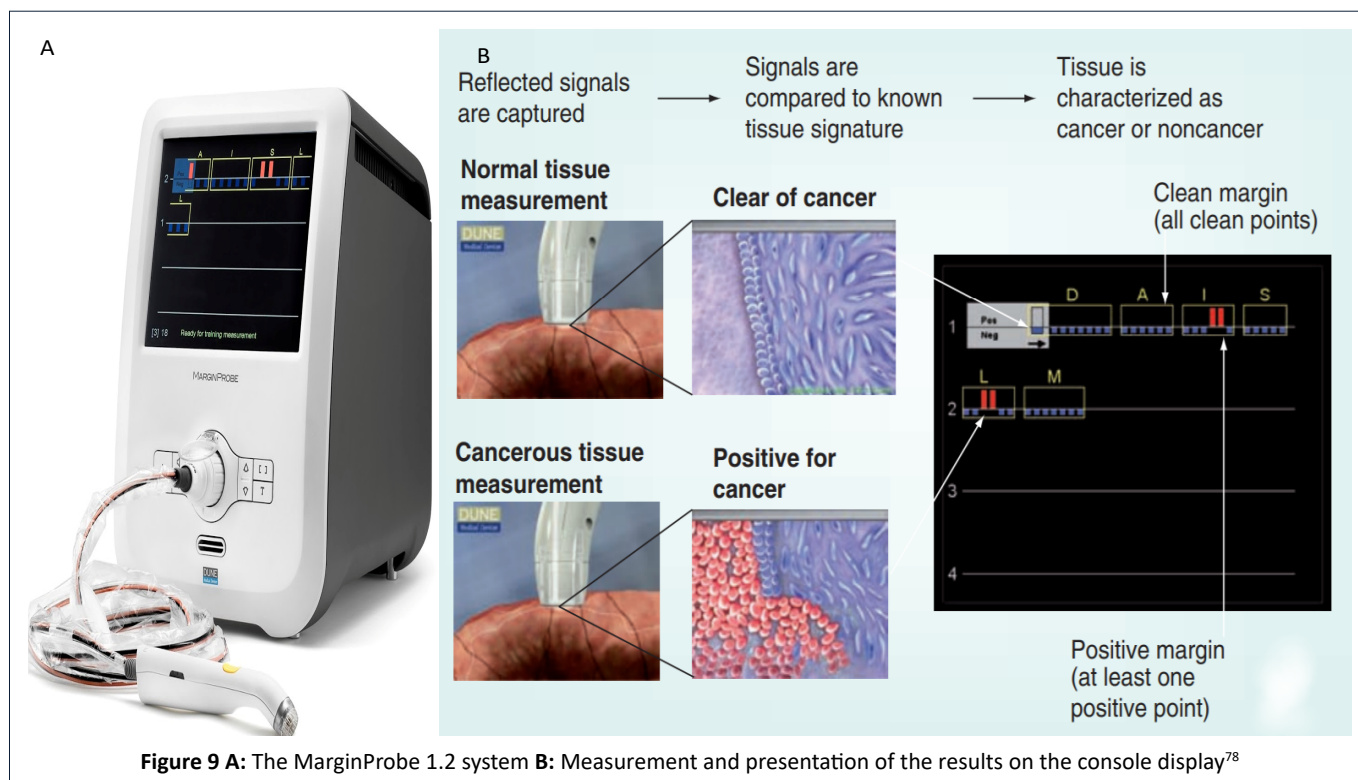


Figure 9 A: The MarginProbe 1.2 system B: Measurement and presentation of the results on the console display<sup>78</sup>

normal (negative). A classification algorithm is applied to obtain the positive/negative results. These results are based on a database of pre-acquired tissue signatures to determine if the tissue is malignant. The console provides a binary representation of the measurement result as seen in figure 9B<sup>78</sup>.

MarginProbe was granted expedited review status. It received premarket approval from the U.S. Food & Drug Administration in 2012. Margin Probe has shown high accuracy for margin assessment in homogeneous ex vivo tumour tissues >6 mm diameter. Pappos et al in their 3-centred study demonstrated a lower accuracy (70% sensitivity and 70% specificity) when probe is used to interrogate regions of multiple tissue types<sup>80</sup>. In Schnabel et al, multi-centred randomized trial with 596 patients, MarginProbe use on excised tissue reduced re-excision rate from 25.8% to 19.8%. Though it suffered from low specificity with a 53.6% false positive rate<sup>81</sup>. This is an indication that relatively high sensitivities come at the cost of relatively greater rates of false positives.

The cost analysis for use in the United States shows that MarginProbe would increase the cost per procedure by \$700 to \$1,700. The device cost between \$10,000 – \$40,000 while the disposable probe costs ~\$1,020.

## Conclusion

The main goal for this review was to identify the gaps in technologies that have been developed for use in breast oncology. This will help academic investigators in consultation with breast cancer clinicians to build upon these innovations. It highlights what is needs to be addressed in the next generation of adjunct technology for breast cancer screening as well as intraoperative margin assessment in BCS. Currently, approximately 20% of BCS patients require repeat surgery due to inadequate margins at the initial operation<sup>82-84</sup>. Positive margins at lumpectomy leads to additional surgeries, treatment delays, significant anxiety for patients, morbidity, poor aesthetic results and increased healthcare costs. These issues will then compromise the advantages of BCS. Extensive resections to obtain negative margins must be balanced to avoid unnecessary removal of normal breast tissue and suboptimal cosmesis<sup>85</sup>. Hematoxylin and eosin histology and immunohistochemistry are currently the clinical gold-standard method for the detection of breast carcinoma and the assessment of protein expression respectively.

The advantage of the iKnife over other emerging technologies such as MarginProbe, ClearEdge or OCT is that oncology workflow is not disrupted, nor an additional probe required during resection or specimen analysis after resection.

The MasSpec Pen ingenuity lies in it being rapid. The entire procedure from triggering the system to data analysis is performed under 10 s The low volume of 10  $\mu$ l or less of high-purity water used causes no impact on analysed tissue. For breast cancer, MasSpec Pen reported ( $n = 45$ ), 87.5% sensitivity, 100% specificity (AUC = 1.0) and overall accuracy of 95.6%<sup>36</sup>. This is comparable to the results reported using DESI-MSI (98.2% accuracy;  $n = 126$ )<sup>38</sup> and the iKnife (95.5% accuracy;  $n = 10$ )[33]. A drawback that will need to be addressed in its use in a larger sampling size, as the degree of precision achieved was with a 1.5 mm sample size.

REMI as a surface imaging technique is appropriate for guiding lumpectomy procedures. It enables full non-destructive imaging of an entire surgical margin surface without the under sampling needed for traditional post-operative histology. However, it is restricted to surface imaging, though many institutions have adopted a “no tumor on ink” criterion for invasive cancers, larger margins are typically desired for *in-situ* cancers. A drawback is the nonspecific accumulation of NPs which is influenced by the mechanical properties of a tissue, such as porosity and interstitial pressure. These properties are often higher in benign tissues compared with dense tumors.

Developing high-performance NIR fluorescence contrast agents to guide surgeons with the guidance during BCS is therefore highly desired. An important concern is that unrelated NIR fluorescence can be generated from other drugs during surgery. An example is Patent Blue (PB) used for sentinel lymph node mapping. PB exhibits a weak NIR fluorescence at 700 nm that could confound the MB results. Vorst et al have previously demonstrated that blue dye can be omitted from sentinel lymph node mapping when indocyanine green (ICG) is used<sup>86</sup>. The FLARE imaging system is also capable of eliminating this potential confounder by imaging 2 independent channels of NIR fluorescence, e.g., NIR Channel 1 for MB-guided breast cancer resection and NIR Channel 2 for ICG-guided sentinel lymph node mapping. It should be possible to also eliminate PB from future protocols. Development of new tumor-specific “800 nm” contrast agents as well as clinically translating them agents for patient care should solve this problem.

OCT, a promising optical technique, is capable of three-dimensional, high-speed and high-resolution imaging. Breast elastography may reduce biopsy of benign lesion. It can be in small form factor probes, making it well-suited for use in operating theatres. The limited ability of OCT to distinguish between tumor and surrounding normal stroma is a reason for its relatively low accuracy. For clinical translation, OCT imaging interpretation time needs to be reduced as well as simplified. Wide-field QME generates three images (OCT, qualitative micro-elastograms, and

quantitative micro-elastograms) which will be difficult to translate real-time in surgery.

Bioimpedance is low cost and non-destructive but requires accurate impedance modelling of the behaviour of the biological system. The CE device is distinctive in its ability to automatically adjust its baseline to the individual patient's heterogeneous breast tissue. Nevertheless, bioimpedance in clinical setting of a heterogeneous cohort, especially obese individuals, subjects with low weight and population groups with unique anthropometric characteristics or in altered states of composition is required<sup>87, 88</sup>. This in effect will enhance bioimpedance detection sensitivity for each individual patient. The CE device also invalidates those hand-held technologies are vulnerable to missing small tumors (e.g., DCIS smaller than 1 mm<sup>2</sup>). This has been argued with respect to spatial resolution and tissue sampling coverage<sup>47</sup>.

Sundar et al in their STAMP study using Fine Needle Aspiration (FNA) samples, demonstrated the technology can be used preoperatively to provide an early indication of disease aggressiveness by mapping the biomarker distribution patterns in cells. Various clinical samples like blood, tissue or urine can be used to generate STAMP barcodes. This can be used to develop a signature library for different diseases. One of its advantages over other protein assays, is its sensitivity. It has the capacity to detect low-abundance proteins at a limit of detection of ~ 10 – 22mol.

MarginProbe, though a new medical technology, does not change the course of follow-up care beyond re-excision nor life expectancy<sup>89</sup>. It cannot be used on shavings or in the lumpectomy cavity of the patient's breast. The device can only be used on the excised tissue. MarginProbe could reduce second lumpectomy surgeries, hence, reducing costs for patients and the health service. This would improve patient's quality of life but then leaves a simple trade-off between cost and the probability of re-excision.

As highlighted earlier, intraoperative pathologic assessment can be performed using frozen section analysis and imprint cytology. But these techniques are resource-intensive, sample only a small percentage of the surgical margins and have limited efficacy especially for DCIS. It is unlikely that techniques that rely on X-rays or ultrasound including intraoperative ultrasound will decrease re-excision rates. Hence, new technology that can be used intraoperatively will have to address this. Greater standardization of the new procedures with higher inter-judge reliability between clinicians is required before any of the innovative technology will be truly "gold standard". However, clinically, the major challenge for these new technologies is in translating and assimilating them into the workflow of an oncological. Further studies will be needed to assess the cost effectiveness of these new technology.

## References

1. World Health Organisation. "WHO | Breast cancer: prevention and control," *Who*, 2016.
2. "Facts and Figures - BREAST CANCER IRELAND." <https://www.breastcancerireland.com/education-awareness/facts-and-figures/> (accessed Jul. 13, 2020).
3. National Cancer Registry. "Cancer projections for Ireland 2015-2040," *Natl. Cancer Regist. Cork*, 2014.
4. Evan GI and Vousden KH. "Proliferation, cell cycle and apoptosis in cancer," *Nature*. 2001, doi: 10.1038/35077213.
5. Kennedy DA, Lee T and Seely D. "A comparative review of thermography as a breast cancer screening technique," *Integrative Cancer Therapies*. 2009, doi: 10.1177/1534735408326171.
6. Hassan AM and El-Shenawee M. "Review of electromagnetic techniques for breast cancer detection," *IEEE Rev. Biomed. Eng.*, 2011, doi: 10.1109/RBME.2011.2169780.
7. NICE. "Recommendations | Early and locally advanced breast cancer: diagnosis and management | Guidance (NG101)," 2020.
8. Pleijhuis RG, Graafland M, De Vries J. "Obtaining adequate surgical margins in breast-conserving therapy for patients with early-stage breast cancer: Current modalities and future directions," *Ann. Surg. Oncol.*, 2009, doi: 10.1245/s10434-009-0609-z.
9. Jacobs L. "Positive margins: The challenge continues for breast surgeons," *Annals of Surgical Oncology*. 2008, doi: 10.1245/s10434-007-9766-0.
10. Miller AR, Brandao G, Prihoda TJ. "Positive/margins following surgical resection of breast carcinoma: Analysis of pathologic correlates," *J. Surg. Oncol.*, 2004, doi: 10.1002/jso.20059.
11. Weng EY, Juillard GJF, Parker RG. "Outcomes and factors impacting local recurrence of ductal carcinoma in situ," *Cancer*, 2000, doi: 10.1002/(SICI)1097-0142(20000401)88:7<1643::AID-CNCR19>3.0.CO;2-O.
12. Park CC, et al., "Outcome at 8 years after breast-conserving surgery and radiation therapy for invasive breast cancer: Influence of margin status and systemic therapy on local recurrence," *J. Clin. Oncol.*, 2000, doi: 10.1200/JCO.2000.18.8.1668.
13. Chagpar AB, Martin RCG, Hagendoorn LJ. "Lumpectomy margins are affected by tumor size and histologic subtype but not by biopsy technique," *Am. J. Surg.*, 2004, doi: 10.1016/j.amjsurg.2004.06.020.
14. Cao D, Lin C, Woo SH. "Separate cavity margin sampling at the time of initial breast lumpectomy significantly reduces the need for reexcisions," *Am. J. Surg. Pathol.*, 2005, doi: 10.1097/01.pas.0000180448.08203.70.
15. Kimball CC, Nichols CI and Vose JG. "The Payer and Patient Cost Burden of Open Breast Conserving Procedures Following Percutaneous Breast Biopsy," *Breast Cancer Basic Clin. Res.*, 2018, doi: 10.1177/1178223418777766.
16. Kennedy KM, et al., "Diagnostic accuracy of quantitative micro-elastography for margin assessment in breast-conserving surgery," *Cancer Res*, 2020, doi: 10.1158/0008-5472.CAN-19-1240.
17. Krekel NMA, et al., "Intraoperative ultrasound guidance for palpable breast cancer excision (COBALT trial): A multicentre, randomised controlled trial," *Lancet Oncol.*, 2013, doi: 10.1016/S1470-2045(12)70527-2.
18. Ramos M, et al., "Ultrasound-guided excision combined with intraoperative assessment of gross macroscopic margins decreases the rate of reoperations for non-palpable invasive breast cancer," *Breast*, 2013, doi: 10.1016/j.breast.2012.10.006.
19. Ahmed M and Douek M. "Intra-operative ultrasound versus wire-

- guided localization in the surgical management of non-palpable breast cancers: systematic review and meta-analysis," *Breast cancer research and treatment*. 2013, doi: 10.1007/s10549-013-2639-2.
20. Olsha O, *et al.*, "Resection margins in ultrasound-guided breast-conserving surgery," *Ann. Surg. Oncol.*, 2011, doi: 10.1245/s10434-010-1280-0.
21. Valdes EK, Boolbol SK, Cohen JM, *et al.* "Intra-operative touch preparation cytology; does it have a role in re-excision lumpectomy?," *Ann. Surg. Oncol.*, 2007, doi: 10.1245/s10434-006-9263-x.
22. St John ER, *et al.*, "Rapid evaporative ionisation mass spectrometry of electrosurgical vapours for the identification of breast pathology: Towards an intelligent knife for breast cancer surgery," *Breast Cancer Res.*, 2017, doi: 10.1186/s13058-017-0845-2.
23. Schlaepfer IR, Hitz CA, Gijón MA, *et al.* "Progesterone modulates the lipid profile and sensitivity of breast cancer cells to docetaxel," *Mol. Cell. Endocrinol.*, 2012, doi: 10.1016/j.mce.2012.08.005.
24. Hilvo M, *et al.*, "Novel theranostic opportunities offered by characterization of altered membrane lipid metabolism in breast cancer progression," *Cancer Res.*, 2011, doi: 10.1158/0008-5472.CAN-10-3894.
25. Calligaris D, *et al.*, "Application of desorption electrospray ionization mass spectrometry imaging in breast cancer margin analysis," *Proc. Natl. Acad. Sci. U. S. A.*, 2014, doi: 10.1073/pnas.1408129111.
26. St John ER, Rossi M, Pruski P. "Intraoperative tissue identification by mass spectrometric technologies," *TrAC - Trends in Analytical Chemistry*. 2016, doi: 10.1016/j.trac.2016.05.003.
27. Kriegsmann J, Kriegsmann M, and Casadonte R. "MALDI TOF imaging mass spectrometry in clinical pathology: A valuable tool for cancer diagnostics (review)," *Int. J. Oncol.*, 2015, doi: 10.3892/ijo.2014.2788.
28. Chughtai K and Heeren RMA. "Mass spectrometric imaging for biomedical tissue analysis," *Chem. Rev.*, 2010, doi: 10.1021/cr100012c.
29. Hsu CC and Dorrestein PC. "Visualizing life with ambient mass spectrometry," *Current Opinion in Biotechnology*. 2015, doi: 10.1016/j.copbio.2014.07.005.
30. Wu C, Dill AL, Eberlin LS. "Mass spectrometry imaging under ambient conditions," *Mass Spectrometry Reviews*. 2013, doi: 10.1002/mas.21360.
31. Ferreira C, Alfaro CM, Pirro V. "Desorption Electrospray Ionization Mass Spectrometry Imaging: Recent Developments and Perspectives," *J. Biomol. Tech.*, 2019.
32. Schäfer KC, *et al.*, "In vivo, in situ tissue analysis using rapid evaporative ionization mass spectrometry," *Angew. Chemie - Int. Ed.*, 2009, doi: 10.1002/anie.200902546.
33. Balog J, *et al.*, "Intraoperative tissue identification using rapid evaporative ionization mass spectrometry," *Sci. Transl. Med.*, 2013, doi: 10.1126/scitranslmed.3005623.
34. Fatou B, *et al.*, "In vivo Real-Time Mass Spectrometry for Guided Surgery Application," *Sci. Rep.*, 2016, doi: 10.1038/srep25919.
35. Schäfer KC, *et al.*, "In situ, real-time identification of biological tissues by ultraviolet and infrared laser desorption ionization mass spectrometry," *Anal. Chem.*, 2011, doi: 10.1021/ac102613m.
36. Zhang J, *et al.*, "Nondestructive tissue analysis for ex vivo and in vivo cancer diagnosis using a handheld mass spectrometry system," *Sci. Transl. Med.*, 2017, doi: 10.1126/scitranslmed.aan3968.
37. Sakai K, *et al.*, "Composition and turnover of phospholipids and neutral lipids in human breast cancer and reference tissues," *Carcinogenesis*, 1992, doi: 10.1093/carcin/13.4.579.
38. Guenther S, *et al.*, "Spatially resolved metabolic phenotyping of breast cancer by desorption electrospray ionization mass spectrometry," *Cancer Res.*, 2015, doi: 10.1158/0008-5472.CAN-14-2258.
39. Carels N, Spinassé LB, Tilli TM. "Toward precision medicine of breast cancer," *Theoretical Biology and Medical Modelling*. 2016, doi: 10.1186/s12976-016-0035-4.
40. Raman CV and Krishnan KS, "A new type of secondary radiation [11]," *Nature*. 1928, doi: 10.1038/121501c0.
41. Haka AS, Shafer-Peltier KE, Fitzmaurice M. "Diagnosing breast cancer by using Raman spectroscopy," *Proc. Natl. Acad. Sci. U. S. A.*, 2005, doi: 10.1073/pnas.0501390102.
42. Hanlon EB, *et al.*, "Physics in Medicine & Biology Prospects for in vivo Raman spectroscopy Prospects for in vivo Raman spectroscopy," *Phys. Med. Biol.*, 2000.
43. Wang YW, *et al.*, "Rapid ratiometric biomarker detection with topically applied SERS nanoparticles," *TECHNOLOGY*, 2014, doi: 10.1142/s2339547814500125.
44. Wang Y, *et al.*, "Raman-encoded molecular imaging with topically applied SERS nanoparticles for intraoperative guidance of lumpectomy," *Cancer Res.*, 2017, doi: 10.1158/0008-5472.CAN-17-0709.
45. Mallia RJ, McVeigh PZ, Fisher CJ, *et al.* "Wide-field multiplexed imaging of EGFR-targeted cancers using topical application of NIR SERS nanoprobe," *Nanomedicine*, 2015, doi: 10.2217/nnm.14.80.
46. Sundah NR, *et al.*, "Barcoded DNA nanostructures for the multiplexed profiling of subcellular protein distribution," *Nat. Biomed. Eng.*, 2019, doi: 10.1038/s41551-019-0417-0.
47. Shipp DW, Rakha EA, Koloydenko AA, *et al.* "Intra-operative spectroscopic assessment of surgical margins during breast conserving surgery," *Breast Cancer Res.*, 2018, doi: 10.1186/s13058-018-1002-2.
48. Troyan SL, *et al.*, "The FLARE™ intraoperative near-infrared fluorescence imaging system: A first-in-human clinical trial in breast cancer sentinel lymph node mapping," *Ann. Surg. Oncol.*, 2009, doi: 10.1245/s10434-009-0594-2.
49. Gioux S, Choi HS, and Frangioni JV. "Image-guided surgery using invisible near-infrared light: Fundamentals of clinical translation," *Molecular Imaging*. 2010, doi: 10.2310/7290.2010.00034.
50. De Grand AM and Frangioni JV. "An Operational Near-Infrared Fluorescence Imaging System Prototype for Large Animal Surgery," *Technol. Cancer Res. Treat.*, 2003, doi: 10.1177/153303460300200607.
51. Tagaya N, *et al.*, "Intraoperative identification of sentinel lymph nodes by near-infrared fluorescence imaging in patients with breast cancer," *Am. J. Surg.*, 2008, doi: 10.1016/j.amjsurg.2007.02.032.
52. Vahrmeijer AL, Hutteman M, Van Der Vorst JR, *et al.* "Image-guided cancer surgery using near-infrared fluorescence," *Nature Reviews Clinical Oncology*. 2013, doi: 10.1038/nrclinonc.2013.123.
53. Bin Xu H, Li L, and Xu Q. "Tc-99m sestamibi scintimammography for the diagnosis of breast cancer: Meta-analysis and meta-regression," *Nuclear Medicine Communications*. 2011, doi: 10.1097/MNM.0b013e32834b43a9.
54. Kim SJ, Kim IJ, Bae YT, *et al.* "Comparison of early and delayed quantified indices of double-phase 99mTc MIBI scintimammography in the detection of primary breast cancer," *Acta radiol.*, 2005, doi: 10.1080/02841850510020752.
55. O'Connor M, Rhodes D and Hruska C. "Molecular breast imaging," *Expert Review of Anticancer Therapy*. 2009, doi: 10.1586/ERA.09.75.
56. Schaafsma BE, *et al.*, "The clinical use of indocyanine green as a near-infrared fluorescent contrast agent for image-guided oncologic surgery," *Journal of Surgical Oncology*. 2011, doi: 10.1002/jso.21943.

57. Tummers QRJG, *et al.*, "Real-time intraoperative detection of breast cancer using near-infrared fluorescence imaging and Methylene Blue," *Eur. J. Surg. Oncol.*, 2014, doi: 10.1016/j.ejso.2014.02.225.
58. Tanaka E, Chen FY, Flaumenhaft R, *et al.* "Real-time assessment of cardiac perfusion, coronary angiography, and acute intravascular thrombi using dual-channel near-infrared fluorescence imaging," *J. Thorac. Cardiovasc. Surg.*, 2009, doi: 10.1016/j.jtcvs.2008.09.082.
59. Nakayama A, Bianco AC, Zhang CY, *et al.* "Quantification of brown adipose tissue perfusion in transgenic mice using near-infrared fluorescence imaging," *Mol. Imaging*, 2003, doi: 10.1162/153535003765276273.
60. Mieog JSD, *et al.*, "Toward optimization of imaging system and lymphatic tracer for near-infrared fluorescent sentinel lymph node mapping in breast cancer," *Ann. Surg. Oncol.*, 2011, doi: 10.1245/s10434-011-1566-x.
61. Millet I, *et al.*, "Invasive breast carcinoma: Influence of prognosis and patient-related factors on kinetic MR imaging characteristics," *Radiology*, 2014, doi: 10.1148/radiol.13122758.
62. Keereweer S, *et al.*, "Optical image-guided surgery - Where do we stand?," *Molecular Imaging and Biology*. 2011, doi: 10.1007/s11307-010-0373-2.
63. Fung YC and Skalak R. "Biomechanics. Mechanical Properties of Living Tissues," *J. Appl. Mech.*, 1982, doi: 10.1115/1.3162171.
64. Kennedy KM, *et al.*, "Diagnostic Accuracy of Quantitative Micro-Elastography for Margin Assessment in Breast-Conserving Surgery," doi: 10.1158/0008-5472.CAN-19-1240.
65. Wojcinski S, *et al.*, "Multicenter study of ultrasound real-time tissue elastography in 779 cases for the assessment of breast lesions: Improved diagnostic performance by combining the BI-RADS®-US classification system with sonoelastography," *Ultraschall der Medizin*, 2010, doi: 10.1055/s-0029-1245282.
66. Xu H, Varghese T, Jiang J, *et al.* "In vivo classification of breast masses using features derived from axial-strain and axial-shear images," *Ultrason. Imaging*, 2012, doi: 10.1177/0161734612465520.
67. Wang RK, Ma Z, and Kirkpatrick SJ. "Tissue Doppler optical coherence elastography for real time strain rate and strain mapping of soft tissue," *Appl. Phys. Lett.*, 2006, doi: 10.1063/1.2357854.
68. Muthupillai R, Rossman PJ, Lomas DJ, *et al.* "Magnetic resonance imaging of transverse acoustic strain waves," *Magn. Reson. Med.*, 1996, doi: 10.1002/mrm.1910360214.
69. Zysk AM, Nguyen FT, Oldenburg AL, *et al.* "Optical coherence tomography: a review of clinical development from bench to bedside," *J. Biomed. Opt.*, 2007, doi: 10.1117/1.2793736.
70. Allen WM, *et al.*, "Wide-field quantitative micro-elastography of human breast tissue," *Biomed. Opt. Express*, 2018, doi: 10.1364/boe.9.001082.
71. Kennedy BF, *et al.*, "Investigation of optical coherence microelastography as a method to visualize cancers in human breast tissue," *Cancer Res.*, 2015, doi: 10.1158/0008-5472.CAN-14-3694.
72. Nguyen FT, *et al.*, "Intraoperative evaluation of breast tumor margins with optical coherence tomography," *Cancer Res.*, 2009, doi: 10.1158/0008-5472.CAN-08-4340.
73. Kassanos P, Constantinou L, Triantis IF, *et al.* "An integrated analog readout for multi-frequency bioimpedance measurements," *IEEE Sens. J.*, 2014, doi: 10.1109/JSEN.2014.2315963.
74. Khan S, Mahara A, Hyams ES, *et al.* "Prostate cancer detection using composite impedance metric," *IEEE Trans. Med. Imaging*, 2016, doi: 10.1109/TMI.2016.2578939.
75. Maglioli CC, Caldwell DG and Mattos LS. "A bioimpedance sensing system for in-vivo cancer tissue identification: Design and preliminary evaluation," *Proc. Annu. Int. Conf. IEEE Eng. Med. Biol. Soc. EMBS*, 2017, doi: 10.1109/EMBC.2017.8037791.
76. Shell J and Gregory WD. "Efficient cancer detection using multiple neural networks," *IEEE J. Transl. Eng. Heal. Med.*, 2017, doi: 10.1109/JTEHM.2017.2757471.
77. Dixon JM, *et al.*, "Intra-operative assessment of excised breast tumour margins using ClearEdge imaging device," *Eur. J. Surg. Oncol.*, 2016, doi: 10.1016/j.ejso.2016.07.141.
78. Thill M and K. Baumann. "New technologies in breast cancer surgery," *Breast Care*. 2012, doi: 10.1159/000343660.
79. Thill M. "MarginProbe®: Intraoperative margin assessment during breast conserving surgery by using radiofrequency spectroscopy," *Expert Rev. Med. Devices*, 2013, doi: 10.1586/erd.13.5.
80. Pappo I, *et al.*, "Diagnostic Performance of a Novel Device for Real-Time Margin Assessment in Lumpectomy Specimens," *Journal of Surgical Research*. 2010, doi: 10.1016/j.jss.2009.02.025.
81. Schnabel F, *et al.*, "A randomized prospective study of lumpectomy margin assessment with use of marginprobe in patients with nonpalpable breast malignancies," *Ann. Surg. Oncol.*, 2014, doi: 10.1245/s10434-014-3602-0.
82. Landercasper J, *et al.*, "Toolbox to Reduce Lumpectomy Reoperations and Improve Cosmetic Outcome in Breast Cancer Patients: The American Society of Breast Surgeons Consensus Conference," *Ann. Surg. Oncol.*, 2015, doi: 10.1245/s10434-015-4759-x.
83. Landercasper J, Whitacre E, Degnim AC, *et al.* "Reasons for Re-Excision After Lumpectomy for Breast Cancer: Insight from the American Society of Breast Surgeons MasterySM Database," *Ann. Surg. Oncol.*, 2014, doi: 10.1245/s10434-014-3905-1.
84. McCahill LE, *et al.*, "Variability in reexcision following breast conservation surgery," *JAMA - J. Am. Med. Assoc.*, 2012, doi: 10.1001/jama.2012.43.
85. Schwarz J and Schmidt H. "Technology for Intraoperative Margin Assessment in Breast Cancer," *Ann. Surg. Oncol.*, vol. 27, no. 7, pp. 2278-2287, 2020, doi: 10.1245/s10434-020-08483-w.
86. Van Der Vorst JR, *et al.*, "Randomized comparison of near-infrared fluorescence imaging using indocyanine green and 99m technetium with or without patent blue for the sentinel lymph node procedure in breast cancer patients," *Ann. Surg. Oncol.*, 2012, doi: 10.1245/s10434-012-2466-4.
87. Naranjo-Hernández D, Reina-Tosina J and Min M. "Fundamentals, recent advances, and future challenges in bioimpedance devices for healthcare applications," *Journal of Sensors*. 2019, doi: 10.1155/2019/9210258.
88. Wingo BC, Barry VG, Ellis AC, *et al.* "Comparison of segmental body composition estimated by bioelectrical impedance analysis and dual-energy X-ray absorptiometry," *Clin. Nutr. ESPEN*, 2018, doi: 10.1016/j.clnesp.2018.08.013.
89. Christian Cuevas PD, *et al.*, "Report of a Pilot Project: Rapid Cost Analyses of Selected Potential High-Impact Intervention Reports," Rockville, MD, 2015.